Desalination and Water Treatment
www.deswater.com
doi: 10.5004/dwt.2021.27387

229 (2021) 227–234
July

Zinc oxide nanoparticles for adsorption of potassium permanganate from wastewater using shaking method

M. Rashad[a,*], S.A. Al-Ghamdi[a], Ahmed Obaid M. Alzahrani[c,d], Khaled Al-Tabaa[a], Safar Al-Osemi[a], Omar Al-Atawi[a], Naser Al-Anzi[a], Shams A.M. Issa[a,e], Alaa M. Abd-Elnaiem[b]

[a]*Nanotechnology Research Laboratory, Department of Physics, Faculty of Science, University of Tabuk, P.O. Box: 741, Tabuk 71491, Saudi Arabia, email: m.ahmad@ut.edu.sa (M. Rashad),*
[b]*Physics Department, Faculty of Science, Assiut University, Assiut 71516, Egypt*
[c]*Center of Nanotechnology, King Abdulaziz University, Jeddah, Saudi Arabia*
[d]*Physics Department, Faculty of Science, King Abdulaziz, University, Jeddah, Saudi Arabia*
[e]*Physics Department, Faculty of Science, Al-Azhar University, Assiut 71452, Egypt*

Received 21 December 2020; Accepted 2 May 2021

ABSTRACT

In this framework, nanostructured zinc oxide (ZnO) adsorbents were formed using the solid-solid reaction method. The crystal structure and morphology of ZnO were investigated using the X-ray powder diffraction and scanning electron microscopy techniques. The ZnO crystallized in the hexagonal close-packed (hcp) structure, while the average crystallite size and particle size were found equal to 22 ± 5 and 55 ± 10 nm, respectively. The adsorption efficiency of the ZnO nanoparticles (NPs) for removing an extreme quantity of potassium permanganate ($KMnO_4$) in wastewater was investigated. The absorbance analysis was revealed that the adsorption of $KMnO_4$ dye reached ~32% in 140 min using the ZnO adsorbent by applying the shaking method. The experimental results were tested by different kinetic models such as pseudo-first as well as pseudo-second-order, and intra-particle diffusion models. Besides, various models including the Boyd and Elovic models are applied to investigate the mechanisms of the removal of $KMnO_4$ from the wastewater using the shaking method. The adsorption process is described well with the pseudo-second-order model for ZnO NPs compared to other applied models. The performance of using ZnO NPs for removing the $KMnO_4$ from the wastewater using the shaking method was compared to other dyes and removal methods found in the literature.

Keywords: ZnO; $KMnO_4$; Nanoparticles; Wastewater; Shaking method

1. Introduction

It is well-known that water covers most of the earth's surface (around 71%). Protection of water to be clean is required for both humans, animals, and plants. The toxic wastewater, as well as the infected waters, are the main subjects that scientists and researchers work on to find friendly environmental solutions. These days, water contamination becomes a serious problem as more than 2% of dyes produced from industries and factories are discharged directly into aqueous effluent [1]. Synthetic dyes are being one of the main reasons for water contamination and environmental pollution, and their extensive application can cause serious health hazards [2,3]. Azoic dyes are considered more than 50% of textile dyes, and such dyes are recognized by nitrogen p-bound [4,5]. It is assessed that over

* Corresponding author.

700,000 tons of dyes and pigments are created every year around the world, and about 1%–20% of world dye items go into material wastewater during the process of dyeing [6–8]. The basic organic processes of the debasement and discoloration on current dyes are insufficient on account of the serious level of aromatic groups in dyes, resulting in different ecological issues [7,8]. The material, paper, food, corrective, and leather goods industries are largely significant consumers of tri-phenyl-methane dyes [9]. The common actual strategies, for example, utilizing filtration, activated carbon, invert osmosis, and coagulation is expensive; and hence do not corrupt the dye, but simply change its phase [10,11]. Alternatively, progressed oxidation measures have been created to manage the issue of dyes pulverization in aqueous systems. The explores illustrate that advanced oxidation processes dependent on photocatalysts are effective. Moreover, this technique has organic compound mineralization. Since the industry likewise utilizes a significant measure of water in the cycles to shape exceptionally shaded industry effluent which has hazardous effect in our biological system because of the presence of these natural synthetics. So, it was important to find another approach to eliminate colored dyes before releasing them into the climate [12,13]. Numerous processes have been proposed for taking out contaminations dye, for example, reverse osmosis, adsorption, nano filtration, electrochemical methods, biodegradation, etc. [14–19]. The different customary advances utilized currently in the evacuation of colored effluents in industrial water are old-style and do not prompt the devastation of the dyes. These strategies do not work efficiently because of the high dissolvability of dyes; accordingly, they simply move the impurities starting from one phase to another [18]. Hence, there is a need to build up a novel treatment technique that is more effective in eliminating dyes. New processes, such as serious oxidative and advanced oxidation are attractive processes. Progressed oxidation measures are elective procedures for destructing dyes in industrials. They were created to satisfy the expanding need for an effective treating of wastewater. These processes are dependent on the development of the firmly oxidizing hydroxyl radicals (OH^-) [20].

Nowadays, expanding nanotechnology usages in various fields still doubt the effect the NPs on the environment. For example, Agarwal et al. [21] reported on the removal of noxious Ni^{+2} using composites of γ-Al_2O_3 nanoparticles and multi-walled carbon nanotubes. Similarly, photocatalytic degradation of amoxicillin from pharmaceutical wastewater using NiO nanoparticle catalysts is investigated [22]. The kinetics, thermodynamics, and isotherm investigation through the adsorptive removal of nitrate from aqueous environments using CuO nanoparticle catalysts are reported [23]. Besides, in our recent work, we have used the shaking method with the presence of some adsorbent and catalysts such as NiO, and CuO nanoparticle catalysts for removing wastes such as methyl orange ($C_{14}H_{14}N_3NaO_3S$) from polluted water [24]. Potassium permanganate ($KMnO_4$) can be used as an oxidizing agent for cyanide compounds, the pharmaceutical industry, and for environmental health safety and water treatment [25,26]. Although the usage of $KMnO_4$ for water treatments (e.g., removal of As and Fe ions), amongst others, there is a need to remove the extraordinary amount of $KMnO_4$ due to its toxicity to non-targeted species in water systems. Mahmoud et al. [27] proposed a method to removing the trace of $KMnO_4$ from the wastewater using the activated carbon modified by various concentrations of H_2SO_4 [27]. Another method such as the photocatalytic degradation process and using ZnO and MgO as a catalyst is applied for removing the $KMnO_4$ from the wastewater [28].

Due to limited studies related to removing $KMnO_4$ from wastewater [27,28], there is a direct goal for using nanoparticles for efficient purification of water after using the oxidizing agents in an extreme quantity such as $KMnO_4$ for water treatment. In this work, ZnO NPs were prepared by the solid–solid reaction method. Also, the contaminated water by an extraordinary amount of $KMnO_4$ (as an example of oxidizing agents) was cleaned by the adsorption technique in the presence of ZnO as an adsorbent. The removal process of the $KMnO_4$ is assisted by the shaking method of the wastewater at various times at room temperature. Moreover, the adsorption efficiency and removal kinetics for the decontamination of contaminated water by $KMnO_4$ were assessed.

2. Experimental details

ZnO NPs were prepared by the solid–solid reaction method at ambient temperature (30°C). For this purpose, 0.2 M $ZnCl_2{\cdot}2H_2O$ has been added to 0.5 M NaOH in a crucible. The color of the mixed solutions was gradually changed from bluish to white color through 5–10 min revealing the formation of the white color of ZnO NPs. Then, the product was carefully washed using distilled water in the furnace for 15 min.

The crystal structure of the prepared ZnO was investigated using a Shimadzu XD-3A X-ray diffractometer (Japan) with monochromatized CuK_α radiation (λ = 1.5418 Å). The surface morphology of ZnO was evaluated using a scanning electron microscopy (SEM) Model SEM-JOEL unit.

The adsorption process of ZnO NPs was carried out using $KMnO_4$ as waste material. A 1,000 mL volume of $KMnO_4$ solution was prepared then diluted to a required concentration of the used solutions. A fixed amount of ZnO NPs (2 mg) was used. The prepared solution was sonicated for 10 min, then transferred to a shaking instrument model (Lab. Tech) for different times over 2 h. The bottle was shacked at a constant rotation speed of 150 rpm. The UV-visible spectrophotometer model Jenway 6300 was used to measure the absorbance at the wavelength range of 200–1,100 nm at room temperature.

3. Results and discussions

Fig. 1a shows the XRD chart of the as-prepared ZnO that was prepared by the solid–solid reaction method. All observed diffraction peaks revealed that the formed ZnO crystallized in the hcp crystal structure. The average estimated crystallite size using the well-known Scherrer equation is around 22 ± 5 nm. More details such as the crystallite size, Miller indices of the diffraction peaks, strain, and dislocation are determined elsewhere [28]. Fig. 1b shows the top-view of SEM for the ZnO sample. It is generally

observed that ZnO particles are spherical with an average estimated particle size 55 ± 10 nm calculated using the ImageJ software program. The estimated particle size confirms that the formed ZnO is in nanoscale which well agrees with our previous study [28].

Fig. 2 shows the absorbance spectra versus wavelength (λ) during the removal of $KMnO_4$ using ZnO NPs as an adsorbent at various shaking times (up to 140 min). It is generally observed from the relationship between absorbance and λ, a presence of two distinct maxima located at λ equals 524 and 545 nm which are characterizing the absorbance of $KMnO_4$. Besides, the radiation absorption through $KMnO_4$ solution was decreased with increasing time of shaking. The reduction in the absorbance confirms the assistant of ZnO NPs as an adsorbent for removing the $KMnO_4$ dye and hence the possible purification of the wastewater using the shaking method.

The adsorption or the $KMnO_4$ removal efficiency (η), similar to other dyes such as methylene blue, and methyl orange can be estimated using the following formulas [29]:

$$\eta(\%) = \frac{(C_0 - C_t)}{C_0} \times 100 = \frac{A_0 - A_t}{A_0} \times 100 \quad (1)$$

Here C_0 is the initial concentration of waste, C_t is the residual concentration of the waste after a shaking time (t), A_0 is the initial absorbance of the waste, and A_t is the absorbance of the waste after a fixed shaking time. Fig. 3 shows the efficiency (η) of removing $KMnO_4$ as waste material as a function of shaking time (t) in the presence of ZnO. As illustrated in Fig. 3, the estimated value was significantly increased up to 24% as the shaking time was increased to 40 min, meanwhile, was slightly increased up to 32% for a further increase in the shaking time to 140 min. The achieved values of adsorption efficiency using the shaking method are greater than the degradation of $KMnO_4$

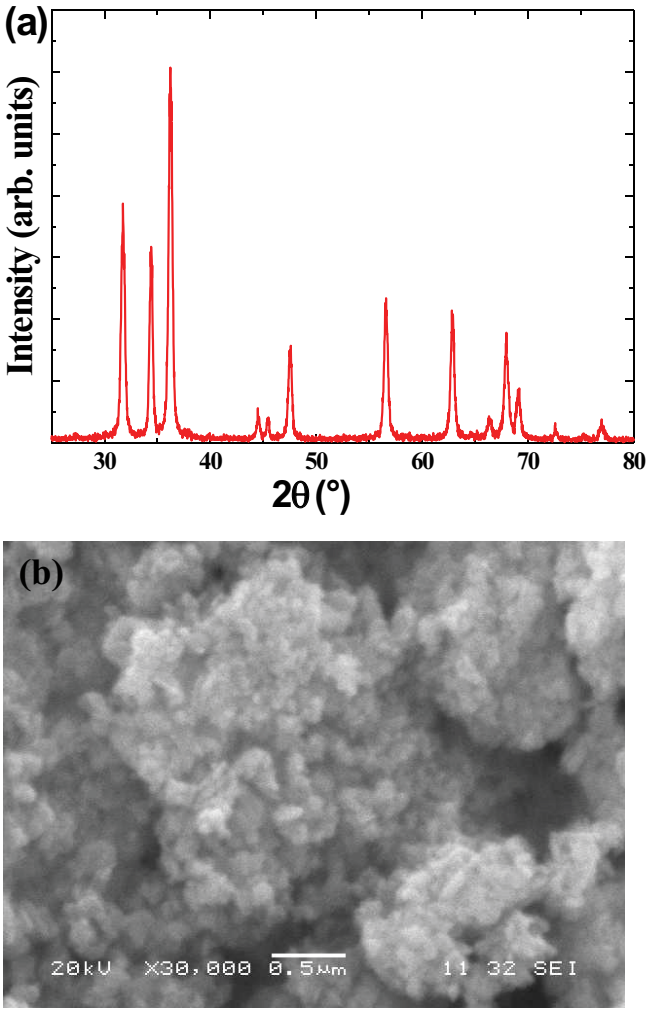

Fig. 1. (a) XRD chart and (b) top-view SEM image of ZnO nanoparticles prepared by solid–solid reaction method.

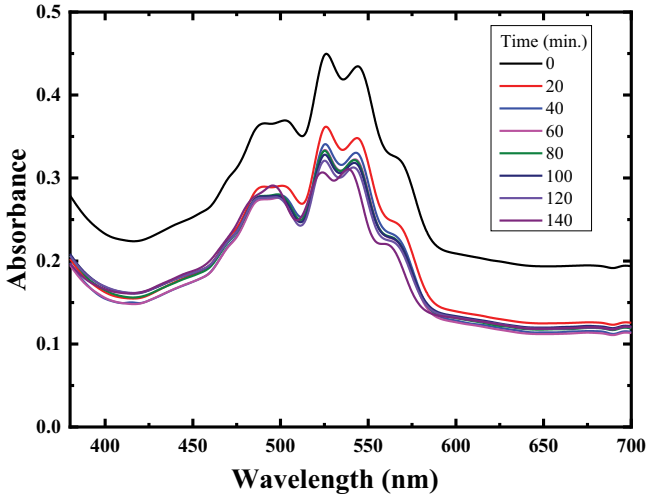

Fig. 2. Absorbance as a function of wavelength (λ) of $KMnO_4$ with ZnO nanoparticles as an adsorbent for various shaking times.

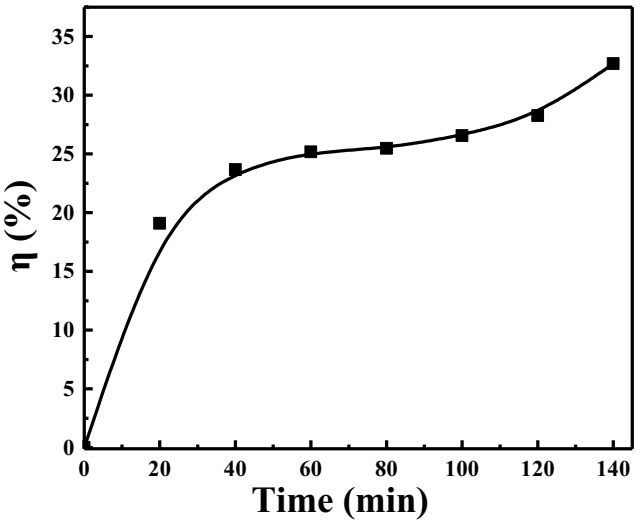

Fig. 3. Adsorption efficiency (η) at various shaking times (t) of $KMnO_4$ debasement using ZnO nanoparticles.

using ZnO (17%) or MgO (25%) catalysts for 3 h [28]. It is worth noting, the adsorptive removal of $KMnO_4$–Mn(II) using modified activated carbon sorbents was changed between 13%, and 100% depending on pH, contacting time, sorbent dose, interfering ions, and the initial concentration of $KMnO_4$ [27].

The adsorbed masses of $KMnO_4$ per unit mass of ZnO NPs (q in mg/g) at any shaking time and equilibrium were calculated by Eqs. (2) and (3), respectively [30]:

$$q_t = \left(C_i - C_t\right)\frac{V}{W} \tag{2}$$

$$q_e = \left(C_i - C_e\right)\frac{V}{W} \tag{3}$$

where q_t is the quantities adsorbed of $KMnO_4$ at a time (t), q_e is the equilibrium quantities adsorbed of $KMnO_4$, C_i is the initial $KMnO_4$ concentration solution (mg/L), C_t is the adsorbate concentrations (mg/L) at a shaking time (t), C_e is the equilibrium adsorbate concentrations (mg/L), V is the adsorbate volume of $KMnO_4$ solution (L), ~25 mL, and W is the adsorbent mass (g). Fig. 4 shows the dependence of q_t of $KMnO_4$ using ZnO as an adsorbent at various shaking times. It was observed that there is an enhancement of q_t as a function of shaking time. The behavior that describes the relation between q_t and t, is quite similar to the relation between η and t. The observed behavior of both mentioned relations reveals the increase of the computed adsorption efficiency which agrees with the previous studies [24,31,32].

Various models were utilized for analyzing the kinetics of the adsorption experimental data such as the intra-particle diffusion kinetic, the pseudo-first-order, and the pseudo-second-order models can be presented as follows [33,34]:

$$q_t = k_{\text{diff}}\sqrt{t} + C \tag{4}$$

$$\log\left(q_e - q_t\right) = \log\left(q_e\right) = \frac{k_1}{2.303}t \tag{5}$$

$$\frac{t}{q_t} = \frac{1}{k_2 q_e^2} + \frac{t}{q_e} \tag{6}$$

where k_{diff} is the intraparticle diffusion kinetic model (mg/g min)$^{1/2}$, k_1 and k_2 are the pseudo-first- and the pseudo-second-order (g/mg min), respectively, and C is the kinetic parameter constant.

The obtained data are plotted based on Eqs. (4)–(6) as shown in Figs. 5–7, respectively. The value of various k_1, k_2, and k_{diff} were estimated.

These values as well as the values of experimental $q_{e,\text{exp}}$ and association coefficients (R^2) values are evaluated and listed in Table 1. The relation between q_t and (t), for the degradation process for $KMnO_4$ using ZnO NPs is presented by a straight line as shown in Fig. 5. From the fitted line, both values of k_{diff} and C for ZnO NPs are estimated. The plot has a correlation coefficient (R^2) value of around 0.90. Therefore, these results indicate that the intra-particle diffusion kinetic model could be suitable for describing the adsorption mechanism (in the present study) for the adsorption of $KMnO_4$ onto ZnO NPs. The estimated value of k_{diff} and C is 3.62 mg/min$^{1/2}$ g, and 5.1, respectively, for adsorption of $KMnO_4$ onto ZnO NPs as listed in Table 1. This assigns that the adsorption of $KMnO_4$ on ZnO NPs has been directed by a single step.

From these outcomes, it is acquired an understanding of these outcomes with those which are accounted for in the literature [35]. Fig. 6 shows the possible applicability of the pseudo-first-order kinetic model for $KMnO_4$ adsorption on the existence of ZnO NPs. Fig. 6 shows a linear relation between $\log(q_e - q_t)$ and t which in agreement with Eq. (5), and accordingly the value of k_1 can be determined from the slope of the fitted line.

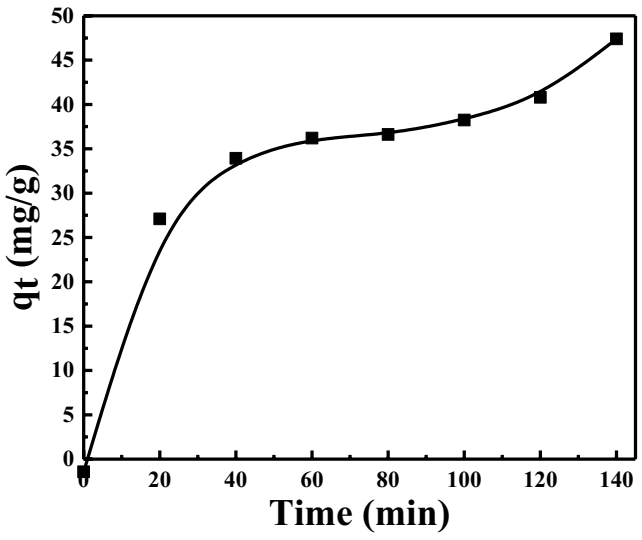

Fig. 4. Adsorption capacity (q_t) of $KMnO_4$ versus shaking time (t) on the ZnO nanoparticles.

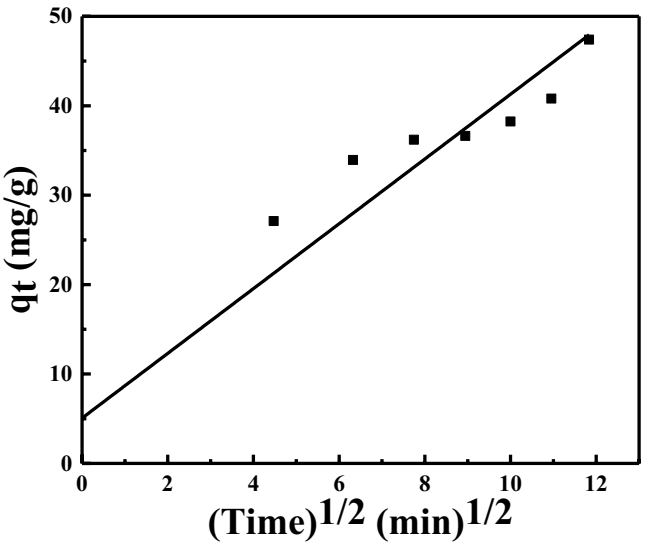

Fig. 5. Intra-particle diffusion model for $KMnO_4$ adsorption on ZnO nanoparticles.

The estimated value of k_1 was found to be equal to 1.4×10^{-2}, while the value of q_e equals 32 mg/g as listed in Table 1. The plotted relation between $\log(q_e - q_t)$ and t has a correlation value $R^2 = 0.85$. Similarly, Fig. 7 illustrates the pseudo-second-order kinetic model for $KMnO_4$ adsorption on the ZnO NPs. It illustrates a linear plot for the relation of t/q_t against t. As shown in Table 1, intercept of the fitted lines, the value of k_2 is obtained and equals 1.8×10^{-3} g/mg min while q_e equals 46 mg/g. In the pseudo-second-order kinetic model, the coefficient of correlation (R^2) equals 0.96 which is greater than the evaluated value for the pseudo-first-order kinetic model (0.85). According to the correlation value, the best model that could be used to describe the adsorption mechanism is the pseudo-second-order kinetic model when compared to the other models. Or by other words, the experiment and calculated values of q_t are closer for pseudo-second than for pseudo-first, as shown in Table 1.

Another proposed equation for studying the adsorption of the investigated sample is called the Elovic equation. The mentioned equation, Eq. (7), is usually applied in chemisorption kinetics of gases on solids. Besides, it can be used for investigating the adsorption of solutes from a liquid solution. The Elovic equation is presented in the following expression [36]:

$$q_t = \frac{\ln(\alpha\beta) + \ln(t)}{\beta} \tag{7}$$

where α is the initial sorption rate (mg/g min), β is the parameter of surface coverage and activation energy for

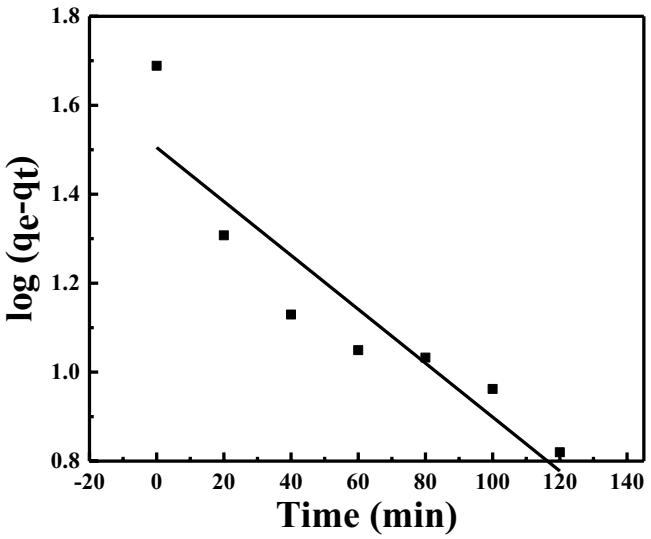

Fig. 6. Pseudo-first-order kinetic model for $KMnO_4$ adsorption on the ZnO nanoparticles.

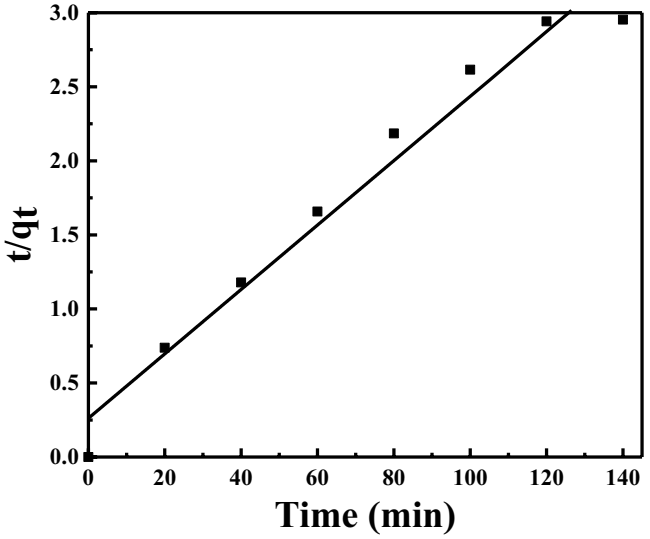

Fig. 7. Pseudo-second-order kinetic model for $KMnO_4$ adsorption on the ZnO nanoparticles.

Table 1
$KMnO_4$ adsorption parameters on ZnO NPs

Pseudo-first-order kinetic model	$q_{e,exp}$ (mg/g)	47
	$q_{e,cal}$ (mg/g)	32
	$q_{e,exp} - q_{e,cal}$	15
	k_1 (min^{-1})	1.4×10^{-2}
	R^2	0.85
Pseudo-second-order kinetic model	$q_{e,cal}$ (mg/g)	45.9
	$q_{e,exp} - q_{e,cal}$	1.1
	k_2 (g/mg min)	1.8×10^{-3}
	R^2	0.96
Intra-particle diffusion kinetic model	K_{eff} ($mg/min^{1/2}$ g)	3.6
	C	5.1
	R^2	0.90
Elovic kinetic model	α (mg/g min)	9.75
	β (g/mg)	0.12
Langmuir–Hinshelwoodmodel	k_{app} (min^{-1})	2.8×10^{-2}

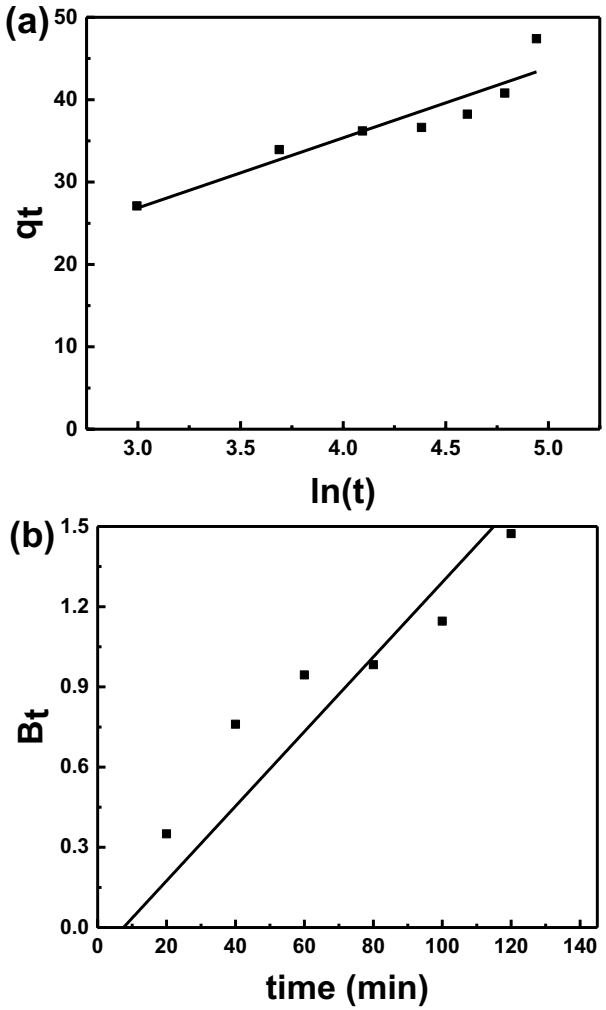

Fig. 8. Plot of (a) q_t versus ln(t), and (b) B_t versus the shaking time (t) during the adsorption of $KMnO_4$ in the presence of ZnO nanoparticles.

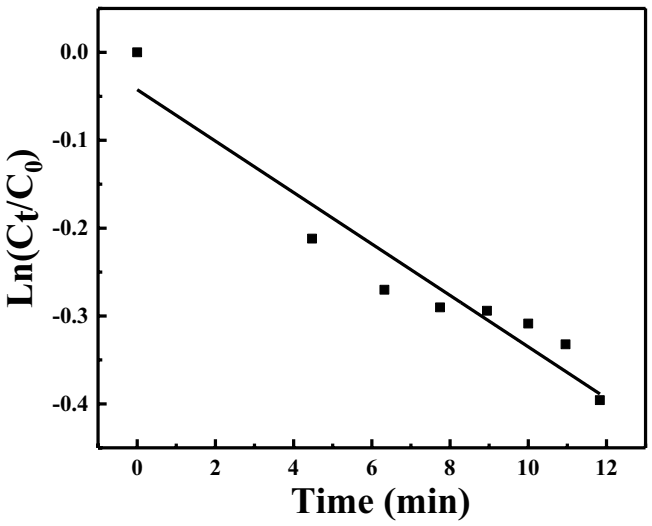

Fig. 9. Semi-logarithmic graph of $KMnO_4$ concentration versus shaking time in the presence of ZnO nanoparticles.

chemisorption (g/mg). β shows the relation between q_t and ln(t) which shows a linear curve for the plotted data and hence the good agreement with Elovic kinetic model. The estimated value of α and β for the adsorption of $KMnO_4$ in the presence of ZnO NPs equals 9.75 mg/g min and 0.12 g/mg, respectively, as listed in Table 1.

It is generally known that the adsorption process could be described through various steps such as (i) solution bulk transport, (ii) film diffusion, (iii) particle diffusion, and (iv) particle and solid's surface sorption and desorption [37]. The processes (ii), and (iii) are called the rate-limiting processes while happening rapidly. Boyd et al. [38] suggested a model be applied for investigating the diffusion mechanism during the adsorption process, which is mathematically written as follows:

$$B_t = -0.4977 - \ln\left(1 - \frac{q_t}{q_e}\right) \tag{8}$$

Eq. (8) is a mathematical function of (q_t/q_e), and this ratio gives the adsorbate adsorbed fraction at various shaking times. According to the model of Boyd, in the case that a linear plot of B_t versus t passes through the origin. It means that the diffusion of particle process is in process control. On the other case, the diffusion could be considered as the rate-limiting step of the process.

The relation between B_t versus t presented in Fig. 8b and the plotted data illustrates a straight line that approximately passes through the origin which means the particle diffusion process is in control and the process is the dominant mechanism.

For more investigating for the adsorption activity of ZnO NPs, the constants of degradation rate $KMnO_4$ debasement were ascertained using the well-known Langmuir–Hinshelwood kinetics. The pseudo-first-order degrading rate response is given from the following equation [39]:

$$\ln\left(\frac{C_t}{C_0}\right) = -kKt = -k_{app}t \tag{9}$$

where k is the degradation rate, K is the adsorption equilibrium, and k_{app} is the apparent rate kinetic constants.

Fig. 9 shows the plot of ln(C_t/C_0) versus the shaking time (t). The relation is given by a straight line that well agrees with Eq. (9) and this confirms that the $KMnO_4$ waste followed fundamentally pseudo-first-order kinetics as discussed before in Fig. 6. The determined value of k_{app} was deduced from the slope of the fitted line and equals 2.8 × 10^{-2}/min (as shown in Table 1).

4. Conclusion

ZnO NPs were simply prepared by the solid–solid reaction method and used as an adsorbent for removing $KMnO_4$ dyes using the shaking method. The ZnO was crystallized in the hcp crystal structure, meanwhile, the average crystallite size and particle size were found equal to 22 ± 5 nm, and 55 ± 10 nm, respectively. The adsorption

activity parameters for ZnO NPs on the wastewater by $KMnO_4$ were computed. It is concluded that the adsorption efficiency was 32% for ZnO NPs. Various models such as Boyd and Elovic were applied to study the possible mechanisms through the adsorption process. The best-fit adsorption kinetic has been attained to the pseudo-second-order model and compared to pseudo-first-order and intra-particle diffusion kinetic models. Kinetics studies confirm that $KMnO_4$ adsorption onto ZnO NPs was attributed to the chemisorption process. Moreover, the proposed shaking method could be used efficiently for removing the $KMnO_4$ dye from the wastewater similar to other methods such as the photocatalytic degradation method.

Acknowledgments

The authors extend their appreciation to the Deanship of Scientific Research at the University of Tabuk for funding this work through Research Group RGP-S-1441-0090.

References

[1] M.A. Rauf, I. Shehadeh, A. Ahmed, A. Al-Zamly, Removal of methylene blue from aqueous solution by using gypsum as a low cost adsorbent, World Acad. Sci. Eng. Technol., 55 (2009) 608–613.
[2] A. Malik, M. Rahman, M.I. Ansari, F. Masood, E. Grohmann, Environmental Protection Strategies: An Overview, Springer, Netherlands, 2011, pp. 1–34.
[3] R. Kant, Textile dyeing industry an environmental hazard, Nat. Sci., 4 (2012) 22–26.
[4] S. Song, L. Xu, Z. He, H. Ying, J. Chen, X. Xiao, B. Yan, Photocatalytic degradation of CI Direct Red 23 in aqueous solutions under UV irradiation using $SrTiO_3/CeO_2$ composite as the catalyst, J. Hazard. Mater., 152 (2008) 1301–1308.
[5] J.W. Lee, S.P. Choi, R. Thiruvenkatachari, W.G. Shim, H. Moon, Evaluation of the performance of adsorption and coagulation processes for the maximum removal of reactive dyes, Dyes Pigm., 69 (2006) 196–203.
[6] J. Madhavan, F. Grieser, M. Ashokkumar, Degradation of orange-G by advanced oxidation processes, Ultrason. Sonochem., 17 (2010) 338–343.
[7] A.B. Isaev, Z.M. Aliev, N.K. Adamadzieva, N.A. Alieva, G.A. Magomedova, The photocatalytic oxidation of azo dyes on Fe_2O_3 nanoparticles under oxygen pressure, Nanotechnol. Russ., 4 (2009) 475–479.
[8] A.H. Mahvi, M. Ghanbarian, S. Nasseri, A. Khairi, Mineralization and discoloration of textile wastewater by TiO_2 nanoparticles, Desalination, 239 (2009) 309–316.
[9] D.F. Duxbury, The photochemistry and photophysics of triphenylmethane dyes in solid and liquid media, Chem. Rev., 93 (1993) 381–433.
[10] M. Janus, A.W. Morawski, New method of improving photocatalytic activity of commercial Degussa P25 for azo dyes decomposition, Appl. Catal., B, 75 (2007) 118–123.
[11] S. Kaur, V. Singh, TiO_2 mediated photocatalytic degradation studies of Reactive Red 198 by UV irradiation, J. Hazard. Mater., 141 (2007) 230–236.
[12] C.I. Pearce, J.R. Lloyd, J.T. Guthrie, The removal of colour from textile wastewater using whole bacterial cells: a review, Dyes Pigm., 58 (2003) 179–196.
[13] T. Robinson, G. McMullan, R. Marchant, P. Nigam, Remediation of dyes in textile effluent: a critical review on current treatment technologies with a proposed alternative, Bioresour. Technol., 77 (2001) 247–255.
[14] M.F. Abid, M.A. Zablouk, A.M. Abid-Alameer, Experimental study of dye removal from industrial wastewater by membrane technologies of reverse osmosis and nanofiltration, Iran. J. Environ. Health Sci. Eng., 9 (2012) 17–17.
[15] V.M. Esquerdo, T.M. Quintana, G.L. Dotto, L.A.A. Pinto, Kinetics and mass transfer aspects about the adsorption of tartrazine by a porous chitosan sponge, React. Kinet. Mech. Catal., 116 (2015) 105–117.
[16] E. Brillas, C.A. Martínez-Huitle, Decontamination of waste-waters containing synthetic organic dyes by electrochemical methods. An updated review, Appl. Catal., B, 166 (2015) 603–643.
[17] S.H. Chen, A.S.Y. Ting, Biodecolorization and biodegradation potential of recalcitrant triphenylmethane dyes by *Coriolopsis* sp. isolated from compost, J. Environ. Manage., 150 (2015) 274–280.
[18] K.M. Lee, C.W. Lai, K.S. Ngai, J.C. Juan, Recent developments of zinc oxide based photocatalyst in water treatment technology: a review, Water Res., 88 (2016) 428–448.
[19] J.A. Byrne, B.R. Eggins, N.M.D. Brown, B. McKinney, M. Rouse, Immobilisation of TiO_2 powder for the treatment of polluted water, Appl. Catal., B, 17 (1998) 25–36.
[20] A.R. Ribeiro, O.C. Nunes, M.F.R. Pereira, A.M.T. Silva, An overview on the advanced oxidation processes applied for the treatment of water pollutants defined in the recently launched Directive 2013/39/EU, Environ. Int., 75 (2015) 33–51.
[21] S. Agarwal, I. Tyagi, V.K. Gupta, M.H. Dehghani, J. Jaafari, D. Balarak, M. Asif, Rapid removal of noxious nickel(II) using novel γ-alumina nanoparticles and multiwalled carbon nanotubes: kinetic and isotherm studies, J. Mol. Liq., 224 (2016) 618–623.
[22] D. Balarak, F.K. Mostafapour, Photocatalytic degradation of amoxicillin using UV/Synthesized NiO from pharmaceutical wastewater, Indonesian J. Chem., 19 (2019) 211–218.
[23] E. Bazrafshan, A.H. Mahvi, M. Havangi, A.H. Panahi, D. Balarak, Adsorptive removal of nitrate from aqueous environments by cupric oxide nanoparticles: kinetics, thermodynamics and isotherm studies, Fresenius Environ. Bull., 27 (2018) 5669–5678.
[24] A.A.A. Darwish, M. Rashad, H.A. AL-Aoh, Methyl orange adsorption comparison on nanoparticles: isotherm, kinetics, and thermodynamic studies, Dyes Pigm., 160 (2019) 563–571.
[25] M. Ordiales, D. Fernández, L.F. Verdeja, J. Sancho, Potassium permanganate as an alternative for gold mining wastewater treatment, JOM, 67 (2015) 1975–1985.
[26] N. Abdullah, H. Abdul Aziz, N.N.A.N. Yusuf, M. Umar, S.S. Abu Amr, Potential of $KMnO_4$ and H_2O_2 in treating semi-aerobic landfill leachate, Appl. Water Sci., 4 (2014) 303–309.
[27] M.E. Mahmoud, A.A. Yakout, S.R. Saad, M.M. Osman, Removal of potassium permanganate from water by modified carbonaceous materials, Desal. Water Treat., 57 (2016) 15559–15569.
[28] M. Rashad, Performance efficiency and kinetic studies of water purification using ZnO and MgO nanoparticles for potassium permanganate, Opt. Quantum Electron., 51 (2019) 1–13.
[29] H. Zhu, R. Jiang, Y. Fu, Y. Guan, J. Yao, L. Xiao, G. Zeng, Effective photocatalytic decolorization of methyl orange utilizing TiO_2/ZnO/chitosan nanocomposite films under simulated solar irradiation, Desalination, 286 (2012) 41–48.
[30] F. Ahmad, W.M.A.W. Daud, M.A. Ahmad, R. Radzi, Using cocoa (*Theobroma cacao*) shell-based activated carbon to remove 4-nitrophenol from aqueous solution: kinetics and equilibrium studies, Chem. Eng. J., 178 (2011) 461–467.
[31] M. Rashad, N.M. Shaalan, A.M. Abd-Elnaiem, Degradation enhancement of methylene blue on ZnO nanocombs synthesized by thermal evaporation technique, Desal. Water Treat., 57 (2016) 26267–26273.
[32] M. Rashad, H.A. AL-Aoh, Promising adsorption studies of bromophenol blue using copper oxide nanoparticles, Desal. Water Treat., 139 (2019) 360–368.
[33] Y.S. Ho, G. McKay, Pseudo-second-order model for sorption processes, Process Biochem., 34 (1999) 451–465.
[34] S. Lagrergen, Zur theorie der sogenannten adsorption gelöster stoffe, Kungl. Svens. Vetenskapsakad. Handl., 24 (1898) 1–39.

[35] H.A. Al-Aoh, M.J. Maah, R. Yahya, M.R. Bin Abas, A comparative investigation on adsorption performances of activated carbon prepared from coconut husk fiber and commercial activated carbon for acid red 27 dye, Asian J. Chem., 25 (2013) 9582–9590.
[36] Y. Bulut, Z. Tez, Adsorption studies on ground shells of hazelnut and almond, J. Hazard. Mater., 149 (2007) 35–41.
[37] G. Akkaya, A. Özer, Biosorption of Acid Red 274 (AR 274) on *Dicranella varia*: determination of equilibrium and kinetic model parameters, Process Biochem., 40 (2005) 3559–3568.
[38] G.E. Boyd, A.W. Adamson, L.S. Myers Jr., The exchange adsorption of ions from aqueous solutions by organic zeolites. II. Kinetics, J. Am. Chem. Soc., 69 (1947) 2836–2848.
[39] H. Yan, J. Hou, Z. Fu, B. Yang, P. Yang, K. Liu, M. Wen, Y. Chen, S. Fu, F. Li, Growth and photocatalytic properties of one-dimensional ZnO nanostructures prepared by thermal evaporation, Mater. Res. Bull., 44 (2009) 1954–1958.